Voltage Support Control Strategies for Static Synchronous Compensators Under Unbalanced Voltage Sags

Miguel Castilla, Jaume Miret, *Member, IEEE*, Antonio Camacho, José Matas, and Luis García de Vicuña

***Abstract*—Static synchronous compensators have been broadly employed for the provision of electrical ac network services, which include voltage regulation, network balance, and stability improvement. Several studies of such compensators have also been conducted to improve the ac network operation during unbalanced voltage sags. This paper presents a complete control scheme intended for synchronous compensators operating under these abnormal network conditions. In particular, this control scheme introduces two contributions: a novel reactive current reference generator and a new voltage support control loop. The current reference generator has as a main feature the capacity to supply the required reactive current even when the voltage drops in amplitude during the voltage sag. Thus, a safe system operation is easily guaranteed by fixing the limit required current to the maximum rated current. The voltage control loop is able to implement several control strategies by setting two voltage set points. In this paper, three voltage support control strategies are proposed, and their advantages and limitations are discussed in detail. The two theoretical contributions of this paper have been validated by experimental results. Certainly, the topic of voltage support is open for further research, and the control scheme proposed in this paper can be viewed as an interesting configuration to devise other control strategies in future works.**

***Index Terms*—Power quality, reactive power control, static synchronous compensator (STATCOM), voltage sag.**

I. Introduction

THE TRADITIONAL configuration of the electrical ac network is nowadays changing. High penetration of renewable energy sources, located close to the point of power consumption, is noticed in recent years [1]. With small transmission and distribution distances, power losses are clearly reduced. In addition, the reduction of the network congestion, the improvement of local power quality, and the provision of ancillary services are notable advantages of the present distributed power generation scenario [2]. Reactive power exchange with the ac network is one of the ancillary services provided by the distributed renewable energy sources. This service can be used to greatly increase the margin to voltage collapse and, thus, to improve the stability of the electrical network. Reactive power is also employed for voltage regulation, network balance, and voltage support during transient abnormal conditions [3]–[8].

Distributed renewable energy sources with low rated power traditionally use reactive power control to govern directly the power factor of the installation. As the generation capacity rises, voltage control is the preferred choice since the ability of these high power sources to influence the terminal voltage increases in this case. The evolution of grid codes for wind power plants clearly illustrates this idea. Most of the previous and current grid codes consider wind power plants as marginal energy sources and specify reactive power (current) injection requirements [9]. Some grid codes that require voltage control have recently emerged as the penetration of wind power is growing significantly. In these codes, the voltage regulation is linked with the reactive power injection normally by means of $V-Q$ curves [10]. In a future scenario, where the penetration of the distributed power plants will be high enough to replace some conventional power generators, the voltage regulation should be carried out by positioning the terminal voltage at a predefined level. This operation will overcome the traditional steady-state error observed in the droop $V-Q$ voltage control.

The capacity of reactive power compensation by renewable energy sources is limited. These sources, interfaced by power inverters, are mainly conceived to export all available active power; thus, the power rating of the inverters is easily achieved. In addition to energy sources, constant power loads can also supply reactive power to the electrical network [11]. Interfaced by active rectifiers, these widely used loads absorb constant active power from the ac network. However, they can exchange only a small amount of reactive power according to the power rating of the active rectifier [12], [13]. As an interesting alternative to renewable energy sources and constant power loads, static synchronous compensators (STATCOMs) can also be regarded as fast voltage–ampere (VA) sources. In fact, STATCOMs are grid-connected voltage source converters (VSCs) normally dedicated to reactive power injection. Active power is consumed in the STATCOM during the system start-up (to charge an internal dc-side capacitor). In the steady state, the active power absorption is very small, and it is only used to compensate for power losses. Consequently, the VA rating of the STATCOM is generally dedicated to reactive power exchange [14], [15].

Manuscript received July 5, 2012; revised November 3, 2012 and January 18, 2013; accepted March 19, 2013. Date of publication April 5, 2013; date of current version August 9, 2013. This work was supported by the Ministry of Economy and Competitiveness of Spain under Project ENE2012-37667-C02-02.

The authors are with the Department of Electronic Engineering, Technical University of Catalonia, 08800 Barcelona, Spain (e-mail: miquel.castilla@upc.edu).

Digital Object Identifier 10.1109/TIE.2013.2257141

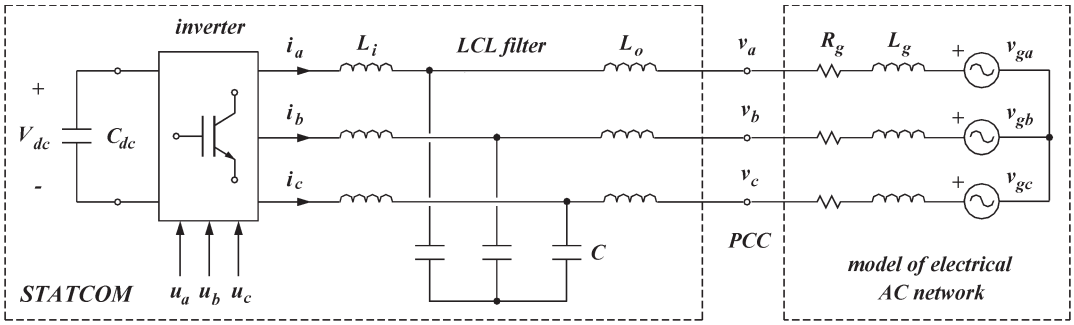

Fig. 1. Diagram of the power system, including the STATCOM and the model of the electrical ac network.

STATCOM technology has been extensively studied and developed in literature [14]–[30]. Investigation of new power circuit topologies that improve the performance of existing configurations was reported in [14]–[18]. Control design issues and performance optimization can be found in [19]–[22]. The operation and integration of the STATCOM in a weak ac network was analyzed in [23]. Most studies, however, focus on the STATCOM operation and performance under abnormal network conditions [24]–[30]. As probably the most severe cause of malfunctioning of grid-connected equipment is unbalanced voltage sags, this is the usual source of abnormal situations considered in these studies. Voltage sags typically tend to deteriorate the performance of the power converters and electrical machines connected to the ac network [26]. In particular, a reduction of the power quality is noticed in this equipment, which is caused by a ripple in the output power and an increase in the current harmonic distortion [27]. Several control schemes have been recently introduced to cope with these problems. Voltage deviations were reduced in the ac network by injecting negative-sequence reactive power in [28]. A coordinated control that supplies both positive-sequence and negative-sequence reactive power was introduced in [29]. This study reveals that it is possible to simultaneously correct the deviation in the positive-sequence voltage and attenuate the negative-sequence voltage to a preset value. In [30], the theoretical limits of the reactive power delivered to the ac network were established in order to ensure that the maximum output current is not exceeded during the voltage sag, thus guaranteeing a safe STATCOM operation. The interesting results presented in this paper were extended in [31] to other reactive power control strategies.

The objective of this paper is to propose a reactive power control scheme for STATCOMs that is able to support the ac network voltage under unbalanced voltage sags. As a first contribution, this paper introduces a new reactive current reference generator, which employs a current set point instead of the usual reactive power set point. The generator has as main feature the capacity to supply the required reactive current even when the voltage drops in amplitude during the voltage sag. Thus, a safe operation is easily obtained by an appropriate design of the current set point. In addition, the control algorithm of the current generator is simple, given that the online calculation of the maximum reactive power delivered to the ac network is not required, as in [30] and [31]. As a second contribution, this paper presents a flexible voltage support control loop with two voltage set points. By setting the values of these set points, different control strategies for voltage support can be devised. In this paper, three strategies are proposed, and their advantages and limitations are discussed in detail. The first strategy sets the set points as in normal network operation. The performance of this strategy during the voltage sag is good enough if the current limit is not reached. Otherwise, the control saturates, and the system operation is clearly deteriorated. As an alternative, two control strategies are thus introduced to cope with this saturation problem.

Section II presents the STATCOM considered in this paper. Section III introduces the new reactive current reference generator. Section IV derives the voltage control scheme and proposes several voltage support control strategies. The advantages and limitations of the proposed strategies are discussed. Section V validates the theoretical contributions by experimental results. Section VI is the conclusion.

II. System Description

This section describes the STATCOM, including the power circuit topology and the control system. In addition, it introduces the basic concepts necessary to study the system.

A. STATCOM

Fig. 1 shows the diagram of the STATCOM considered in this paper. The power circuit topology includes a three-phase VSC, a dc-side capacitor $C_{\rm dc}$, and an LCL output filter. In transmission and distribution power systems, the STATCOM is normally connected to the point of common coupling (PCC) through a step-up transformer. In Fig. 1, inductor L_o represents the leakage inductance of the STATCOM transformer (the magnetizing inductance is not considered here). The electrical network is represented by a grid impedance (R_g and L_g) in series with an ac voltage source. The grid impedance physically models other power system transformers as well as the line impedance. Note that the values of R_g, L_g, and v_g are the reflected quantities to the primary side of the STATCOM transformer.

The voltage at the PCC and the current at the converter side $\mathbf{i}$ are sensed and supplied to the control system. This current is preferred for control purposes instead of the current at the

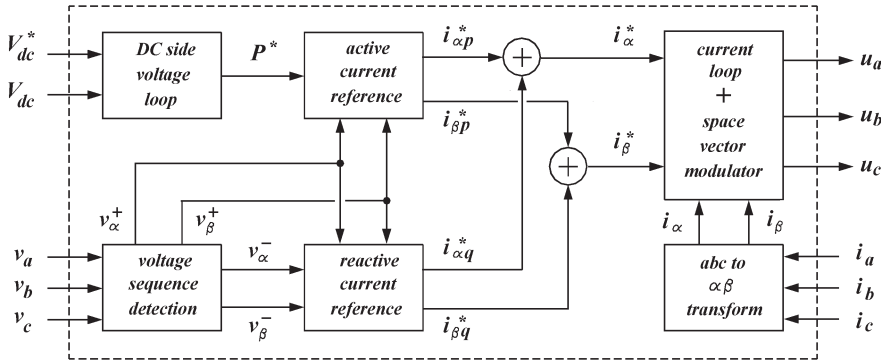

Fig. 2. Diagram of the STATCOM control system.

ac network side (flowing through L_o) due to the improvement achieved in the system robustness [32], [33].

B. Control System

The control system for the STATCOM should provide control input $\mathbf{u}$ in accordance to the following objectives.

1) The capacitor voltage $V_{\rm dc}$ should be regulated to the dc voltage set point $V_{\rm dc}^*$. This ensures the absorption of a small active power from the ac network necessary to compensate for power losses.
2) The maximum current should not be exceeded. A current set point I^* is employed in the control system to perform this task (see Section III).
3) The PCC voltage should be regulated between set points $V_{\max}^*$ and $V_{\min}^*$, which are the maximum and minimum voltages at the PCC, respectively. Three control strategies to set the values for these set points during unbalanced voltage sags are presented and discussed in Section IV.

The previous objectives are accomplished with the control system shown in Fig. 2. The control consists of an external voltage loop, an internal current loop, and a space vector modulator. The internal loop is a tracking regulator designed to provide fast and accurate current control. Proportional and resonant regulators are employed for this task. In the Laplace domain, these compensators are implemented by the following transfer function (both in α and β current channels):

$$H(s) = k_{p,\,c} + \sum_{m=1,\,5,\,7,\,11} \frac{k_{m,\,c} 2\xi_c (m\omega_g) s}{s^2 + 2\xi_c (m\omega_g) s + (m\omega_g)^2} \quad (1)$$

with s being the Laplace operator, $k_{p,\,c}$ being the proportional gain, $k_{m,\,c}$ being the resonant gain, ξ_c being the damping factor, and m being the selected harmonics. Further details about these regulators can be found in [34]–[36].

The external loop is responsible for generating the current references, expressed in (2) and (3), according to the set points $V_{\rm dc}^*$ and I^* as follows:

$$i_\alpha^* = i_{\alpha p}^* + i_{\alpha q}^* \quad (2)$$

$$i_\beta^* = i_{\beta p}^* + i_{\beta q}^* \quad (3)$$

with $i_{\alpha p}^*$ and $i_{\beta p}^*$ and $i_{\alpha q}^*$ and $i_{\beta q}^*$ being the active and reactive current references, respectively. A key element in the external loop is the voltage sequence detector. This detector extracts the positive- and negative-sequence voltages at the PCC as follows:

$$v_\alpha = v_\alpha^+ + v_\alpha^- \quad (4)$$

$$v_\beta = v_\beta^+ + v_\beta^-. \quad (5)$$

These symmetrical voltage components can be defined as

$$v_\alpha^+ = V^+ \cos(\omega t + \varphi^+) \quad (6)$$

$$v_\beta^+ = V^+ \sin(\omega t + \varphi^+) \quad (7)$$

$$v_\alpha^- = V^- \cos(-\omega t - \varphi^-) \quad (8)$$

$$v_\beta^- = V^- \sin(-\omega t - \varphi^-). \quad (9)$$

Note that, in general, amplitudes V^+ and V^-, angular frequency ω, and initial phases φ^+ and φ^- are time-varying signals. These signals can be computed online as

$$V^+ = \sqrt{\left(v_\alpha^+\right)^2 + \left(v_\beta^+\right)^2} \quad (10)$$

$$V^- = \sqrt{(v_\alpha^-)^2 + (v_\beta^-)^2} \quad (11)$$

$$\cos(\varphi^+ - \varphi^-) = \frac{v_\alpha^+ v_\alpha^- - v_\beta^+ v_\beta^-}{V^+ V^-} \quad (12)$$

$$\sin(\varphi^+ - \varphi^-) = \frac{v_\alpha^+ v_\beta^- - v_\beta^+ v_\alpha^-}{V^+ V^-}. \quad (13)$$

Several voltage sequence detectors can be found in literature to extract the above information. In this paper, the detector reported in [37] was employed. It implements a bandpass filter tuned at the fundamental grid frequency to extract in-phase signal v_e and a low-pass filter to obtain in-quadrature signal v_q, in both α and β voltage channels. The filters are frequency adaptive in order to track properly the variable frequency of the grid voltage. The transfer functions of the filters can be written as

$$\frac{v_e(s)}{v(s)} = \frac{2\xi_v \omega_e s}{s^2 + 2\xi_v \omega_e s + \omega_e^2} \quad (14)$$

$$\frac{v_q(s)}{v(s)} = \frac{\omega_e^2}{s^2 + 2\xi_v \omega_e s + \omega_e^2} \quad (15)$$

with ξ_v being the damping factor and ω_e being the estimated grid frequency. It is worth mentioning that this voltage sequence separator gives high harmonic rejection due to its bandpass filter nature [37].

The current supplied to the ac network during unbalanced voltage sags can be highly distorted by harmonics. By using the given sequence detector, together with the following active current references [3], the current harmonics are strongly reduced:

$$i^*_{\alpha p} = \frac{2}{3}\frac{v^+_\alpha}{(V^+)^2}P^* \tag{16}$$

$$i^*_{\beta p} = \frac{2}{3}\frac{v^+_\beta}{(V^+)^2}P^* \tag{17}$$

where P^* is the active power reference. As shown in Fig. 2, this signal is generated by the dc-side voltage loop, which is implemented here as a conventional proportional–integral (PI) regulator.

The reactive current references

$$i^*_{\alpha q} = \frac{2}{3}\frac{k_q v^+_\beta + (1-k_q)v^-_\beta}{k_q(V^+)^2 + (1-k_q)(V^-)^2}Q^* \tag{18}$$

$$i^*_{\beta q} = \frac{2}{3}\frac{-k_q v^+_\alpha - (1-k_q)v^-_\alpha}{k_q(V^+)^2 + (1-k_q)(V^-)^2}Q^* \tag{19}$$

also provide low harmonic distortion when they are employed together with the aforementioned voltage sequence detector. These references, introduced in [8] specifically for voltage support, are the starting point to derive a new reactive current reference generator with a current set point instead of a reactive power set point (see Section III).

In (18) and (19), Q^* is the reactive power reference, and k_q is a control gain that commands the exchange of reactive power in terms of positive and negative sequences. By setting $k_q = 1$, the reactive power is injected via a positive sequence only. With $k_q = 0$, the reactive power is delivered via a negative sequence only. It is possible to combine both symmetrical components by choosing k_q inside the range of $0 < k_q < 1$ [8], [29].

C. Voltage Unbalance Factor

An essential characteristic of the electrical ac network is the voltage unbalance factor. This factor indicates the amount of negative sequence found at the PCC (in relation to the positive sequence). It can be defined as

$$n = \frac{V^-}{V^+}. \tag{20}$$

Ideally $n = 0$, meaning that the network voltage is balanced. In normal conditions, this factor is small, i.e., typically $n < 0.02$ [38]. During unbalanced voltage sags, however, high values of n are expected. The factor is frequently within the range of $0.1 < n < 0.4$, although higher values are also possible [38], [39].

III. Reactive Current Reference Generator

The first contribution of this paper is a reactive current reference generator. This section is devoted to the derivation of this generator. In particular, in this section, the expressions of the reference signals that fix the maximum amplitude of the phase currents to a predefined value (i.e., the set point I^*) are deduced. This objective should also be reached when the phase currents are unbalanced. In addition, at the end of this section, the mechanism of reactive power injection of the proposed current reference generator is revealed through the analysis of the positive- and negative-sequence reactive power.

Note that the injected current could be easily limited to a fixed maximum amplitude by using a standard reactive power control in cascade with a current limiting block. However, in this case, the injected current will be clipped during an over current condition, resulting in an unacceptable total harmonic distortion. As shown in the following, the proposed current generator limits the maximum amplitude to a predefined value without distorting the current waveforms.

As the active power is only employed to compensate for power losses, the active current is negligible in relation to the reactive current. Therefore, only reactive current reference is considered in this section.

A. Maximum Reactive Power Delivered to the AC Network

By inserting (6)–(9) and (20) into (18)–(19), the stationary reference frame current references can be expressed as a function of time. Then, an expression for the phase current references in the natural frame is easily obtained by using the inverse Clarke transformation. The amplitudes of these current references are

$$I^*_x = \frac{2}{3}\frac{\sqrt{k_q^2 - 2nk_q(1-k_q)\cos_x + n^2(1-k_q)^2}}{k_q + n^2(1-k_q)}\frac{Q^*}{V^+} \tag{21}$$

where $x = a$, b, or c, and the function $\cos_x$ can be written as

$$\cos_x = \cos\left(\varphi^+ - \varphi^- + m\frac{2\pi}{3}\right) \tag{22}$$

where $m = 0$, 1, or 2. From (21), it is easy to note that the currents are balanced if the voltage is balanced $(n = 0)$, i.e.,

$$I^*_a = I^*_b = I^*_c = \frac{2}{3}\frac{Q^*}{V^+}. \tag{23}$$

In addition, the currents are balanced (even during unbalanced voltage conditions, $n > 0$) if the control gain $k_q = 1$ or $k_q = 0$. With $k_q = 1$, the current amplitudes satisfy (23). For $k_q = 0$, the current amplitudes can be expressed as

$$I^*_a = I^*_b = I^*_c = \frac{2}{3}\frac{Q^*}{nV^+}. \tag{24}$$

For k_q values inside the range of $0 < k_q < 1$, the currents are unbalanced. In this case, the phase current with higher amplitude should be considered to establish the limits of the reactive power. For this purpose, the current set point I^* is

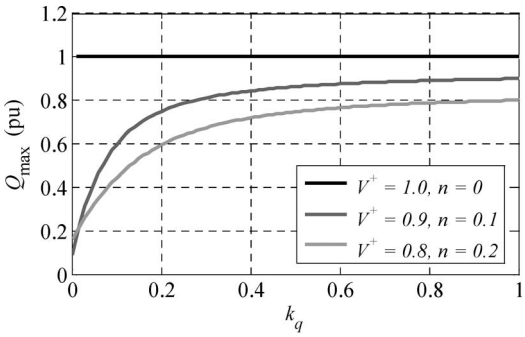

Fig. 3. Maximum reactive power versus control gain k_q and for several values of V^+ and n ($I_{\max} = 1$ p.u., $\cos_{\min} = -0.5$).

defined as the higher phase current amplitude, and from (21), it can be written as

$$I^* = \frac{2}{3}\frac{\sqrt{k_q^2 - 2nk_q(1-k_q)\cos_{\min} + n^2(1-k_q)^2}}{k_q + n^2(1-k_q)}\frac{Q^*}{V^+} \quad (25)$$

where the function $\cos_{\min}$ is

$$\cos_{\min} = \min(\cos_x). \quad (26)$$

Note that the minimum value of (22) is necessary to calculate the current set point (i.e., the maximum phase current) given that the term $2nk_q(1-k_q)\cos_{\min}$ has a negative sign in (25). Thus, the maximum reactive power $Q_{\max}$ injected to the ac network is calculated from (25) by replacing the current set point by the maximum STATCOM rated current $I_{\max}$, i.e.,

$$Q_{\max} = \frac{3}{2}\frac{\left(k_q + n^2(1-k_q)\right)V^+}{\sqrt{k_q^2 - 2nk_q(1-k_q)\cos_{\min} + n^2(1-k_q)^2}} I_{\max}. \quad (27)$$

Note that, although the maximum current $I_{\max}$ is a fixed parameter, the maximum reactive power $Q_{\max}$ varies with the voltage characteristics (V^+, n, and $\cos_{\min}$) and the control gain k_q. This fact can be clearly observed in Fig. 3. This figure shows the loss of power capacity of the STATCOM when the grid voltage is in abnormal conditions ($V^+ < 1$ p.u. and/or $n > 0$). In fact, only for nominal conditions ($V^+ = 1$ p.u. and $n = 0$), the maximum reactive power is 1 p.u., and no power capacity loss is noticed. It is worth mentioning that the maximum power rating is available in abnormal conditions when the reactive power is injected via a positive sequence only (i.e., for $k_q = 1$).

B. Proposed Reactive Current Reference Generator

The reference generator is derived by inserting the reactive power reference from (25) to (18) and (19), resulting in

$$i^*_{\alpha q} = \frac{k_q v^+_\beta + (1-k_q)v^-_\beta}{\sqrt{k_q^2 - 2nk_q(1-k_q)\cos_{\min} + n^2(1-k_q)^2}}\frac{I^*}{V^+} \quad (28)$$

$$i^*_{\beta q} = \frac{-k_q v^+_\alpha - (1-k_q)v^-_\alpha}{\sqrt{k_q^2 - 2nk_q(1-k_q)\cos_{\min} + n^2(1-k_q)^2}}\frac{I^*}{V^+}. \quad (29)$$

Some inputs of (28) and (29) can be calculated online by the voltage sequence detector. The voltage unbalance factor n is obtained by using (10), (11), and (20). The function $\cos_{\min}$ is computed using (12), (13), and (26). Positive- and negative-sequence components of the PCC voltage are directly obtained at the output of the voltage sequence detector, as shown in Fig. 2. However, the two remaining inputs (the set point I^* and the control gain k_q) should be chosen in order to fulfill a specific control objective, as discussed in the following.

The current set point is certainly the maximum amplitude of the phase currents, as can be easily deduced from (21) and (25). Thus, an accurate selection of the current set point is enough to guarantee a safe STATCOM operation, i.e.,

$$0 \le I^* \le I_{\max}. \quad (30)$$

C. Reactive Power Injection

The positive- and negative-sequence reactive power injected to the ac network can be defined as [8]

$$q^+ = \frac{3}{2}\left(-v^+_\alpha i^+_\beta + v^+_\beta i^+_\alpha\right) \quad (31)$$

$$q^- = \frac{3}{2}\left(-v^-_\alpha i^-_\beta + v^-_\beta i^-_\alpha\right). \quad (32)$$

By inserting (6)–(9), (28), and (29) in the given expressions, the reactive power provided by the STATCOM when the proposed reactive current reference generator is used can be written as

$$q^+ = \frac{3}{2}\frac{k_q V^+}{\sqrt{k_q^2 - 2nk_q(1-k_q)\cos_{\min} + n^2(1-k_q)^2}} I^* \quad (33)$$

$$q^- = \frac{3}{2}\frac{n^2(1-k_q)V^+}{\sqrt{k_q^2 - 2nk_q(1-k_q)\cos_{\min} + n^2(1-k_q)^2}} I^*. \quad (34)$$

It is worth mentioning that when the voltage is balanced ($n = 0$) or by setting $k_q = 1$ in case of imbalance voltage ($n > 0$), the reactive power is injected via positive sequence only, i.e.,

$$q^+ = \frac{3}{2}V^+ I^* \qquad q^- = 0. \quad (35)$$

By setting $k_q = 0$ in the case of imbalance voltage, the reactive power is delivered via a negative sequence only, i.e.,

$$q^+ = 0 \qquad q^- = \frac{3}{2}V^- I^*. \quad (36)$$

A combination of both reactive power sequences can be used by choosing k_q inside the range of $0 < k_q < 1$. An interesting application of this flexible power injection mechanism is presented in the following.

IV. Voltage Support Control Strategies

The second contribution of this paper is a voltage support control scheme intended for STATCOMs under unbalanced voltage sags. This section is devoted to the derivation of this

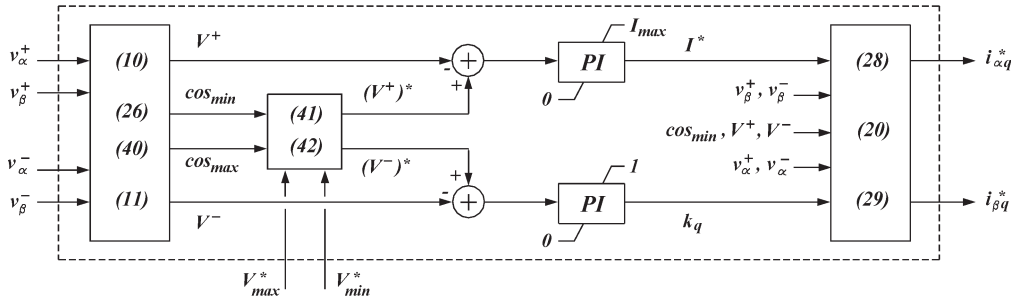

Fig. 4. Diagram of the proposed reactive current reference generator with voltage support auxiliary service.

voltage control. In addition, three voltage support control strategies are introduced and discussed in detail.

A. Control Objectives

The aim of this section is to devise a voltage control loop that provides the values of the set point I^* and the control gain k_q according to the PCC voltage set points $V^*_{\max}$ and $V^*_{\min}$. Then, by setting different values for these voltage set points, several voltage support control strategies can be defined.

From (33) and (34), it is easy to observe that the current set point I^* controls the reactive power delivered to the ac network. In fact, by increasing the current set point, a higher injection of reactive power is achieved, which also increases the positive-sequence voltage at the PCC [29]. Therefore, this set point is employed here to regulate the positive-sequence voltage V^+ to the reference $(V^+)^*$. Moreover, the control gain k_q allows a balanced injection of reactive current through positive and negative sequences. In particular, the negative-sequence voltage at the PCC decreases, by decreasing the value of the gain k_q [29]. As a result, this control gain is used to regulate the negative-sequence voltage V^- to the reference $(V^-)^*$.

According to the given discussion, the diagram of the proposed voltage support control scheme is shown in Fig. 4. It includes the reactive current reference generator derived in Section III and the voltage set-point generator presented in this section. The value of the current set point I^* is generated by a PI regulator, fed by the error between the positive-sequence voltage and its voltage set point. In addition, a PI regulator, fed by the error between the negative-sequence voltage and its voltage set point, produces the value of the control gain k_q. The outputs of these two regulators are limited by the maximum values allowed for these two variables, as shown in Fig. 4. Note that the voltage set points $V^*_{\max}$ and $V^*_{\min}$ are inputs to this control scheme. To complete the implementation of the proposed generator, however, it is necessary to derive the expressions that relate the voltage set points $V^*_{\max}$ and $V^*_{\min}$ with the voltage symmetrical component set points $(V^+)^*$ and $(V^-)^*$. This derivation is carried out in the following.

B. Derivation of Symmetrical Component Set Points

By inserting (6)–(9) into (4) and (5), the stationary reference frame PCC voltages can be expressed as a function of time. Then, an expression for the phase voltages in the natural reference frame is easily obtained by using the inverse Clarke transformation. The amplitude of these voltages can be written as

$$V_x = \sqrt{(V^+)^2 + 2V^+V^- \cos_x + (V^-)^2} \tag{37}$$

where $x = a$, b, or c.

By defining $V_{\max}$ and $V_{\min}$ as the maximum and minimum amplitudes of the phase voltages, respectively, then

$$V_{\max} = \sqrt{(V^+)^2 + 2V^+V^- \cos_{\max} + (V^-)^2} \tag{38}$$

$$V_{\min} = \sqrt{(V^+)^2 + 2V^+V^- \cos_{\min} + (V^-)^2} \tag{39}$$

where $\cos_{\min}$ is defined in (26), and the function $\cos_{\max}$ is

$$\cos_{\max} = \max(\cos_x). \tag{40}$$

Note that (38) and (39) relate phase voltage amplitudes with symmetrical component amplitudes. It is worth mentioning that these expressions are also valid for the voltage set points. Thus, the set points for symmetrical component amplitudes can be deduced from (38) and (39), and they can be written as

$$(V^+)^* = \sqrt{\frac{\mu + \sqrt{\mu^2 - (V^*_{\max})^2 + (V^*_{\min})^2}}{2(\cos_{\max} - \cos_{\min})}} \tag{41}$$

$$(V^-)^* = \frac{(V^*_{\max})^2 - (V^*_{\min})^2}{2(\cos_{\max} - \cos_{\min})(V^+)^*} \tag{42}$$

where

$$\mu = (V^*_{\min})^2 \cos_{\max} - (V^*_{\max})^2 \cos_{\min}. \tag{43}$$

C. Control Strategies

This section proposes three control strategies that can be implemented by the voltage support control scheme shown in Fig. 4.

The first control strategy, known from now on as control strategy 1 (CS1), is devised for nominal ac voltage operation range. In this case, the voltage regulation is ideally achieved by setting the following voltage set points:

$$V^*_{\max} = V_{\text{nom}} \tag{44}$$

$$V^*_{\min} = V_{\text{nom}} \tag{45}$$

where $V_{\rm nom}$ is the nominal voltage. Note that, with these set points, the negative-sequence voltage at the PCC should be completely eliminated. However, due to practical limitations, a certain amount of negative-sequence voltage is accepted at the PCC [27]. Therefore, the voltage set points for CS1 are formulated as

$$V^*_{\rm max} = 1.01 V_{\rm nom} \tag{46}$$

$$V^*_{\rm min} = 0.99 V_{\rm nom}. \tag{47}$$

In abnormal network conditions with significant voltage imbalance, the CS1 is actually a very current-demanding strategy given that high reactive current injection is necessary to completely remove the voltage imbalance. A simple way to reduce the reactive current injection is to set the voltage set points to the limits specified in grid codes for normal operation [10], [40]. This setting defines the second control strategy, known as control strategy 2 (CS2), which can be formulated as

$$V^*_{\rm max} = 1.10 V_{\rm nom} \tag{48}$$

$$V^*_{\rm min} = 0.88 V_{\rm nom}. \tag{49}$$

The third control strategy (CS3) is also devised for ac networks with significant voltage imbalance. However, in this case, the aim is to reduce the negative-sequence voltage beyond the reduction achieved with CS2. This can be obtained by positioning the voltage set points of CS3 between the voltage set points of CS1 and CS2. As an extra feature, this CS3 adjusts the voltage set points dynamically in accordance with the reactive current injection. The dynamic set points for CS3 can be written as

$$V^*_{\rm max} = \left[1.10 - k_{p,I}(I_{\rm max} - I^*)\right] V_{\rm nom} \tag{50}$$

$$V^*_{\rm min} = \left[0.88 + k_{p,I}(I_{\rm max} - I^*)\right] V_{\rm nom} \tag{51}$$

where $k_{p,I}$ is a proportional term gain. Therefore, CS3 can be viewed as an intermediate solution between CS1 and CS2. Note that, when the current set point I^* is coming near to the maximum current $I_{\rm max}$, then CS3 voltage set points approach to CS2 set points [see (48) and (49)]. On the contrary, when the current set point comes close to 0 A, the maximum deviation of CS3 set points is obtained. Obviously, this deviation must be saturated by the limits defined in (46) and (47). Thus, in this situation (low reactive current injection), the CS3 strategy is approaching to the CS1 strategy. To sum up, an adaptive voltage positioning is proposed in (50) and (51), which reduces the negative-sequence voltage at the PCC by setting intermediate voltage set points.

V. Experimental Validation

This section validates the theoretical contributions of this paper by experimental results. Two sets of experiments are reported to confirm the features of the reactive current reference generator and the voltage support control scheme.

TABLE I
PARAMETERS OF THE AC NETWORK AND THE STATCOM

Symbol	Quantity	Nominal value
S_{sc}	AC network short-circuit power	20.4 kVA, 8.743 pu
S_b	STATCOM rated power (base power)	2.33 kVA, 1 pu
V_g	AC network voltage (line to line)	$\sqrt{3}$110 Vrms, 1 pu
V_{nom}	STATCOM nominal voltage (base volt.)	$\sqrt{3}$110 Vrms, 1 pu
$I_{\rm max}$	STATCOM maximum rated current	10 Apeak, 1 pu
f_g	AC network frequency (base frequency)	60 Hz, 1 pu
R_g	grid impedance resistor	125 mΩ, 0.008 pu
L_g	grid impedance inductor	4.7 mH, 0.114 pu
C_{dc}	DC-side capacitor	1.36 mF, 7.976 pu
L_i	LCL inverter side inductor	6.9 mH, 0.167 pu
C	LCL filter capacitor	680 nF, 0.004 pu
L_o	LCL grid side inductor	2.1 mH, 0.051 pu
f_s	switching and sampling frequencies	10 kHz, 166.66 pu

TABLE II
PARAMETERS OF THE PROPOSED CONTROL SCHEMES

Symbol	Quantity	Nominal value
$k_{p,c}$	proportional gain of the current loop	30 V/A
$k_{m,c}$	resonant gain of the current loop	150 V/A
ξ_c	damping factor of the current loop	0.2
ξ_v	damping factor of the sequence detector	0.707
V^*_{dc}	DC-side voltage setpoint	350 V
$k_{p,V_{dc}}$	proportional gain of the V_{dc} voltage loop	0.3 V
$k_{i,V_{dc}}$	integral gain of the V_{dc} voltage loop	15 Vs
k_{p,V^+}	proportional gain of the V^+ voltage loop	0.2 A/V
k_{i,V^+}	integral gain of the V^+ voltage loop	20 A/(Vs)
k_{p,V^-}	proportional gain of the V^- voltage loop	0.01 $(\rm V)^{-1}$
k_{i,V^-}	integral gain of the V^- voltage loop	2 $(\rm Vs)^{-1}$
$k_{p,I}$	proportional gain of the CS3 strategy	0.04 $(\rm A)^{-1}$

A. Experimental Setup

A laboratory prototype of the power system shown in Fig. 1 was build using a Semikron three-phase insulated-gate bipolar transistor inverter and a programmable Pacific Power ac power supply. The nominal values for the power system parameters are listed in Table I. The control system shown in Figs. 2 and 4 was implemented in a TMS320F28335 floating-point digital signal processor from Texas Instruments. The bandwidths of the internal and external control loops were conveniently separated, i.e., 1.2 kHz and 60 Hz, respectively, to avoid undesired interactions. Table II lists the control parameters that fulfill this requirement. The design of these control loops has been carried out by considering the following constraints. For the current loop, the bandwidth is lower than the switching frequency (about a decade below) and higher than 660 Hz, i.e., the frequency of the higher harmonic considered

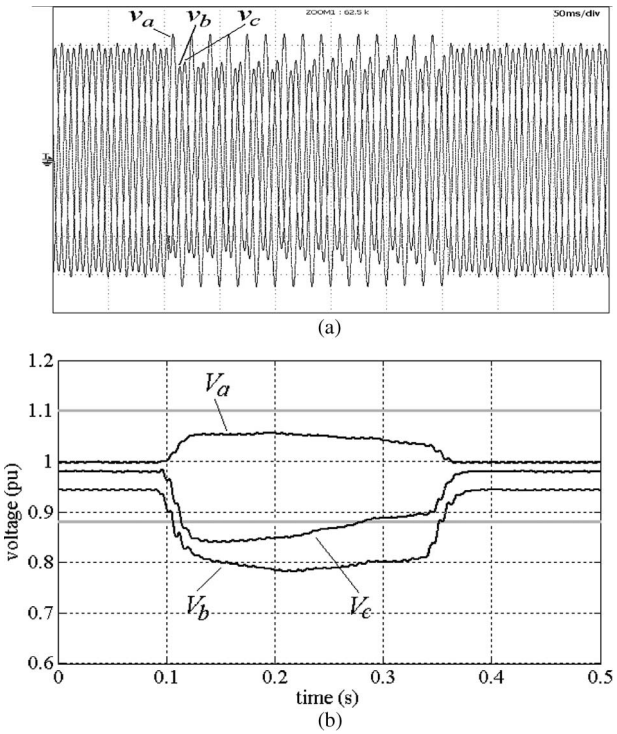

Fig. 5. Voltage at the PCC when the STATCOM was inactive. (a) Instantaneous voltage (50 V/div, 50 ms/div). (b) RMS voltage in p.u.

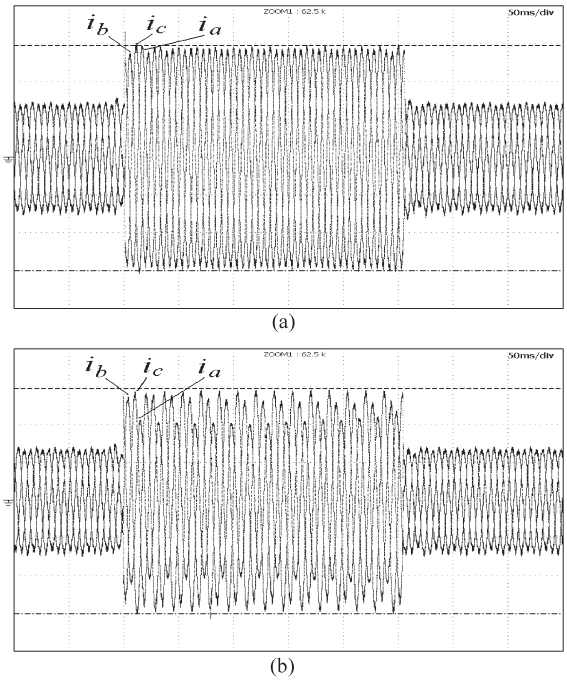

Fig. 6. STATCOM current for fixed set point $I^* = 10$ A (3.33 A/div, 50 ms/div). (a) $k_q = 1$. (b) $k_q = 0.5$.

in the current compensator [see (1)]. For the voltage loop, the bandwidth is lower than (but close to) 200 Hz, i.e., the bandwidth of the voltage sequence detector [37]. With this particular design, the voltage at the PCC has a fast enough transient response and a negligible error in steady state since the voltage sequence detector has enough time to be updated.

The proposed STATCOM was tested with a voltage sag presented in [41]. This event, shown in Fig. 5, has a large steady-state imbalance (see the time interval from 0 to 0.1 s or from 0.35 to 0.5 s) and a variable voltage profile during the transient state (see the time interval from 0.1 to 0.35 s). For this reason, the chosen voltage sag is a good candidate to evaluate the performance of the proposed control solution in adverse stringent network conditions. Fig. 5 shows both instantaneous and RMS voltages. The limits for normal operation specified in grid codes were also depicted in Fig. 5(b) (see gray traces [40]).

B. Tests on the Reactive Current Reference Generator

The first experiments were conduced to evaluate the current reference generator proposed in (28) and (29) under the abnormal ac network condition shown in Fig. 5. For this purpose, the voltage support control loops were disconnected (see Fig. 4), and the current set point was fixed to the maximum rated current, i.e., $I^* = 10$ A. Fig. 6 shows the measured STATCOM current for two fixed values of the control gain k_q. For $k_q = 1$, the reactive current has only positive sequence; thus, the current is balanced. In any case, the peak current during the voltage sag is limited by the current set point, as desired. For $k_q = 0.5$, the reactive current is composed by both positive- and negative-sequence components; thus, the current is unbalanced. In this case, the reference generator also produces a maximum peak current of 10 A. Note that the amplitude of the other phases is changing over time (always with a value lower than the specified rated current) as a result of the variable voltage sag profile.

C. Tests on the Voltage Support Control Strategies

The next set of experiments was conduced to evaluate the voltage support control strategies presented in Section IV. In this case, the voltage control loops shown in Fig. 4 were activated, providing variable values for the current set point I^* and the control gain k_q in accordance with the considered control strategies. The STATCOM operation in steady state and under the voltage sag is illustrated in Figs. 7–9.Three experiments were carried out by using CS1, CS2, and CS3 during the voltage sag, as defined in Fig. 7. Note that, in steady state, the CS1 was employed in the three experiments.

Excellent results were achieved in steady state, as shown in Fig. 7, in comparison with the waveforms depicted in Fig. 5. In fact, when the STATCOM was activated, the voltage at the PCC was inside the range defined by the CS1 voltage set points. This fact can be clearly observed in Fig. 7(d)–(f). (See, in particular, the time interval from 0 to 0.1 s.) As a consequence, the negative-sequence voltage at the PCC was nearly eliminated during steady state with a reactive current of 0.5 p.u. and a control gain $k_q = 0.02$ (see Fig. 8). This corresponds to a positive-sequence reactive power of 0.27 p.u. and a negative-sequence reactive power of 0.02 p.u. (see Fig. 9).

The performance of the proposed control strategies during the voltage sag can be clearly observed in Fig. 7. Poor results were obtained with CS1, as shown in Fig. 7(a) and (d). Note that the voltage at the PCC does not track the voltage set points expressed in (46) and (47) from 0.1 to 0.35 s. In fact, this

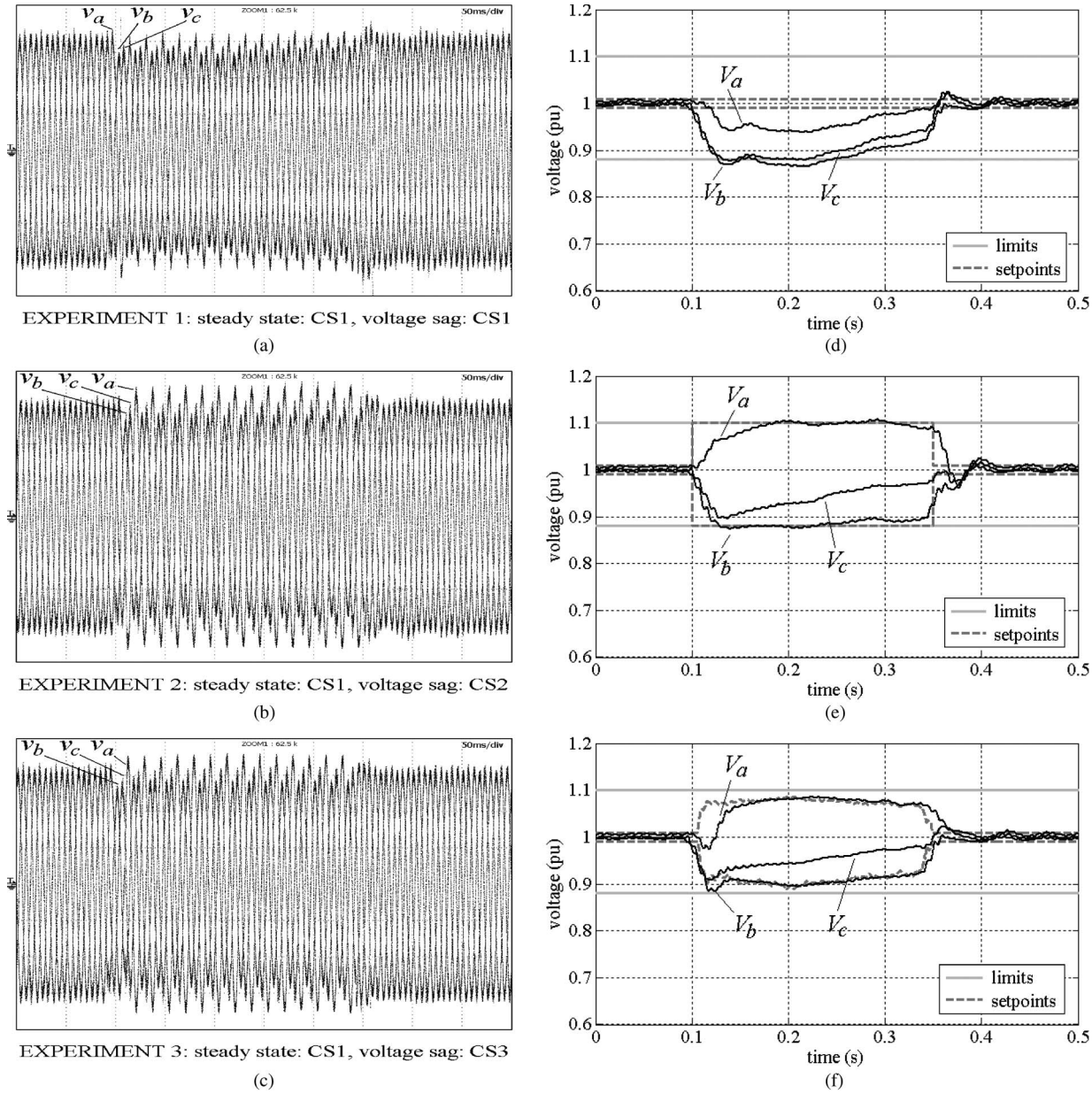

Fig. 7. Voltage at the PCC when the STATCOM was active. (a), (b), and (c) Instantaneous voltage (50 V/div, 50 ms/div) for experiments 1, 2 and 3, respectively. (d), (e) and (f) RMS voltage in p.u. for experiments 1, 2 and 3, respectively.

voltage is even lower than the 0.88-p.u. limit during a certain time interval. This is due to the saturation of the voltage support control loops, as can be observed in Fig. 8(d). Note that the outputs of these loops during the voltage sag are the constant values $I^* = 10$ A and $k_q = 0$, i.e., the upper and lower limits of these variables, respectively. Figs. 8(a) and 9(a) show the STATCOM current and the reactive power delivered to the ac network, respectively, during this transient saturation event of the voltage loops. Quite the opposite, good results were achieved with both CS2 and CS3. As shown in Fig. 7(e), the voltage at the PCC tracks correctly the fixed voltage set points expressed in (48) and (49) for CS2 during the voltage sag. Note that both the higher and lower phase voltages follows the fixed 1.1 p.u. and 0.88 p.u. limits, respectively. A similar result is noticed in Fig. 7(f) when CS3 is used during the voltage sag. In this case, however, the voltage set points are variable, as expressed in (50) and (51), but again, the voltage at the PCC tracks satisfactorily the set points. The most important difference between CS2 and CS3 is the higher reduction of the negative-sequence voltage achieved by this last strategy. This can be observed in Fig. 7(f) by the fact that the highest phase voltage is lower than the 1.1-p.u. limit and the lowest phase voltage is higher than the 0.88-p.u. limit. In that sense, the limits specified in grid codes for normal ac network conditions are accomplished with enough room. It is worth mentioning that the higher reduction of negative-sequence voltage in CS3 is achieved due to both the increase in the reactive current injection [see Fig. 8(b) and (c)] and the reduction in the control gain k_q value [see Fig. 8(e) and (f)]. Note that, although the set point I^* and the gain k_q are continuously evolving during the fault to compensate the variable voltage sag profile, these control variables are not saturated at any time instant when CS2 and

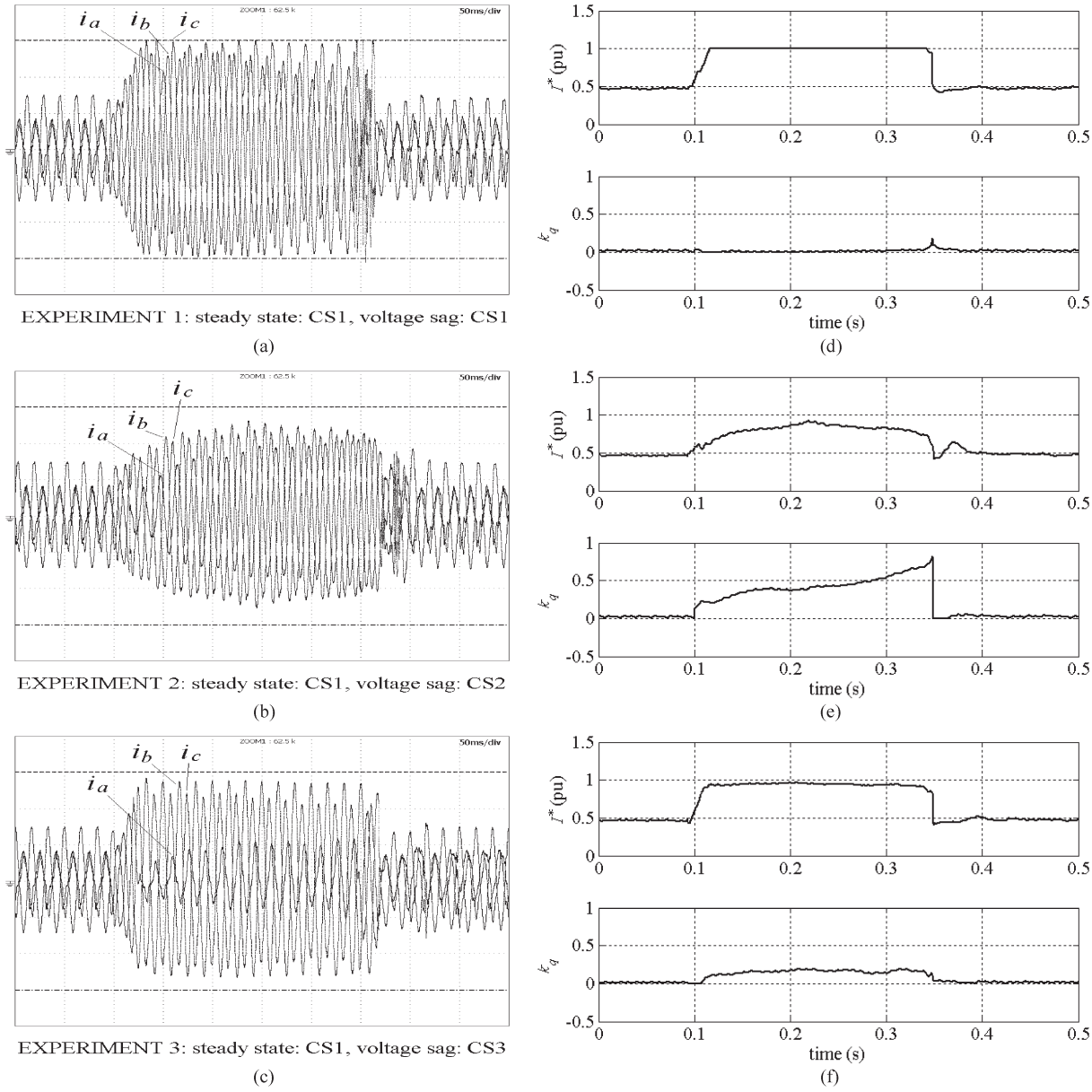

Fig. 8. STATCOM operation in steady state and under the voltage sag. (a), (b), and (c) Instantaneous STATCOM current (3.33 A/div, 50 ms/div) for experiments 1, 2 and 3, respectively. (d), (e), and (f) Outputs of the voltage support control loops for experiments 1, 2, and 3, respectively.

CS3 are employed. By comparing the results shown in Fig. 8(b) and (c), it is interesting to note that the higher reduction of the negative-sequence voltage produced by the CS3 is achieved due to the injection of a higher negative-sequence current. This fact can be noticed in the higher imbalance of the phase currents shown in Fig. 8(c). The reactive power delivered to the ac network with CS2 and CS3 can be observed in Fig. 9(b) and (c). Note that the aforementioned reduction of negative-sequence voltage achieved with CS3 can also be explained by the increase in the negative-sequence reactive power shown in Fig. 9(c).

D. Comparison With the Conventional Scheme of Reactive Power Injection

The grid code [10] states that the generating plants must support the grid voltage with additional reactive power during the voltage sag. The voltage control must take place when the voltage is outside the specified limits by providing a reactive current amounting at least 2% of the rated current for each percentage of the voltage sag. In addition, a reactive power of at least 100% of the rated current must be possible if necessary (for PCC voltages lower than 40%). This specification defines the conventional scheme of reactive power injection by providing the minimum reactive current that must be injected during a voltage sag as a function of the voltage at the PCC.

Fig. 10 shows the total reactive power injected by the proposed voltage support control strategies (i.e. $q_{\rm tot} = q^+ + q^-$) and the reactive power required for the grid code $q_{\rm gc}$ [10]. Note that the injected reactive power $q_{\rm tot}$ is higher than the required reactive power $q_{\rm gc}$ for all the considered strategies (see the results for experiments 1, 2, and 3), thus satisfying the grid code specification during the voltage sag.

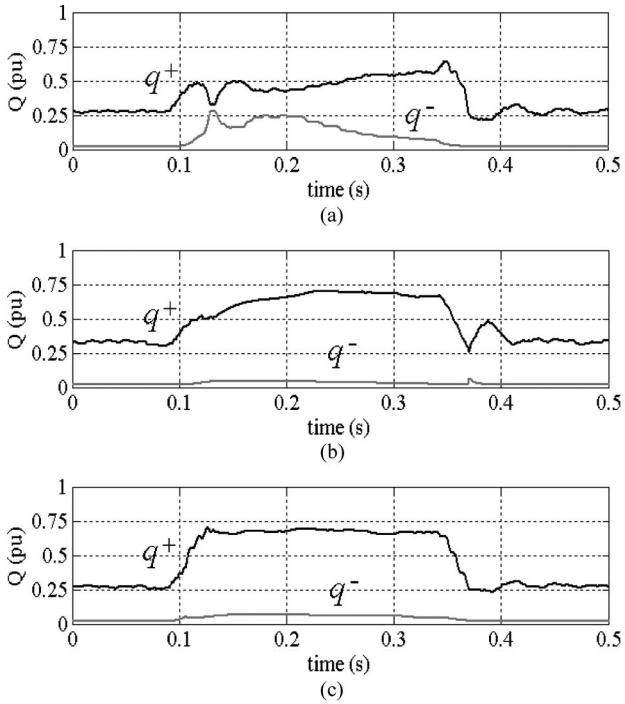

Fig. 9. Positive- and negative-sequence reactive power in p.u. (q^+/S_b and q^-/S_b). (a) Experiment 1. (b) Experiment 2. (c) Experiment 3.

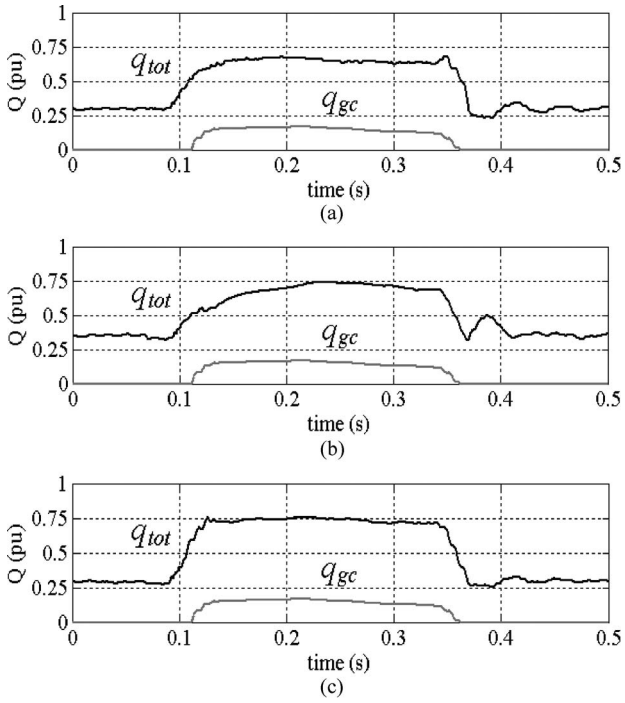

Fig. 10. Injected reactive power for (a) experiment 1, (b) experiment 2, (c) experiment 3, and the reactive power $q_{\rm gc}$ required in grid code [10].

VI. Conclusion

A complete control scheme intended for STATCOMs operating under unbalanced voltage sags has been presented in this paper. The first contribution is a reactive current reference generator programmed with a current set point instead of the conventional reactive power set point. As an interesting feature, this generator guarantees a safe operation of the STATCOM by naturally limiting the amplitude of the current delivered to the ac network. The main advantage in comparison with previous reference generators is that the online calculation of the maximum reactive power is not required since the output limits in the proposed algorithm are constant values even in the presence of grid voltages with imbalances. The second contribution is a voltage control loop that makes possible the introduction of several voltage support control strategies by simply modifying two voltage set points. Three control strategies are proposed to verify the effectiveness of the control scheme under severe unbalanced voltage sags. The CS1 has good results in normal network conditions but has poor results during abnormal conditions with significant voltage imbalance. In fact, a STATCOM with higher power rating is required to supply the necessary reactive current to fulfill the requirements specified by the CS1. The CS3 and CS3 relax the stringent specifications of CS1 and provide good results during the unbalanced voltage sag by changing the position of the voltage set points. The main differences between these strategies are as follows: 1) CS2 requires the minimum injection of reactive current by positioning the voltage set points at the limits specified in grid codes for normal operation; and 2) CS3 achieves the lower negative-sequence voltage at the PCC by adaptively positioning the voltage set points in accordance with the reactive current injection. In that case, the voltage limits are not exceeded with a certain room for security. In comparison with existing voltage control loops based on a voltage-reactive power droop characteristic, the proposed control ensures an accurate voltage regulation to a predefined voltage set point provided that the STATCOM rated power and the impedance of the ac network are large enough. This feature will be particularly appreciated in a future scenario where the penetration of the distributed power plants will be high enough to replace some conventional power generators. Actually, the topic of voltage support control strategies is open for further research, and the synthesis of novel control strategies implemented with the proposed voltage control scheme is left to future work.

References

[1] J. M. Carrasco, L. G. Franquelo, J. T. Bialasiewicz, E. Galván, R. C. Guisado, M. A. Prats, J. I. León, and N. Moreno-Alfonso, "Power-electronic systems for the grid integration of renewable energy sources: A survey," *IEEE Trans. Ind. Electron.*, vol. 53, no. 4, pp. 1002–1016, Jun. 2006.

[2] F. Blaabjerg, R. Teodorescu, M. Liserre, and A. V. Timbus, "Overview of control and grid synchronization for distributed power generation systems," *IEEE Trans. Ind. Electron.*, vol. 53, no. 5, pp. 1398–1409, Oct. 2006.

[3] P. Rodrıacute;guez, A. Timbus, R. Teodorescu, M. Liserre, and F. Blaabjerg, "Independent PQ control for distributed power generation systems under grid faults," in *Proc. IEEE IECON*, 2006, pp. 5185–5190.

[4] A. Luna, P. Rodrıacute;guez, R. Teodorescu, and F. Blaabjerg, "Low voltage ride through strategies for SCIG wind turbines in distributed power generation systems," in *Proc. IEEE PESC*, 2008, pp. 2333–2339.

[5] P. Rodriguez, A. Timbus, R. Teodorescu, M. Liserre, and F. Blaabjerg, "Reactive power control for improving wind turbine system behavior under grid faults," *IEEE Trans. Power Electron.*, vol. 24, no. 7, pp. 1798–1801, Jul. 2009.

[6] F. Wang, J. L. Duarte, and M. A. Hendrix, "Pliant active and reactive power control for grid-interactive converters under unbalanced voltage dips," *IEEE Trans. Power. Electron.*, vol. 26, no. 5, pp. 1511–1521, May 2011.

[7] A. Junyent-Ferré, O. Gomis-Bellmunt, T. C. Green, and D. E. Soto-Sánchez, "Current control reference calculation issues for the operation of renewable source grid interface VSCs under unbalanced voltage sags," *IEEE Trans. Power. Electron.*, vol. 26, no. 12, pp. 3744–3753, Dec. 2011.
[8] A. Camacho, M. Castilla, J. Miret, J. Vasquez, and E. Alarcon-Gallo, "Flexible voltage support control for three phase distributed generation inverters under grid fault," *IEEE Trans. Ind. Electron.*, vol. 60, no. 4, pp. 1429–1441, Apr. 2013.
[9] J. Martinez and P. C. Kjaer, "Fast voltage control in wind power plants," in *Proc. IEEE Power Energy Soc. Gen. Meet.*, 2011, pp. 1–7.
[10] *Grid Code-High and Extra High Voltage*, E. ON Netz GmbH, Bayreuth, Germany, 2006.
[11] M. Molinas, D. Moltoni, G. Fascendini, J. A. Suul, and T. Undeland, "Constant power loads in distributed AC systems: An investigation of stability," in *Proc. IEEE ISIE*, 2008, pp. 1531–1536.
[12] N. Jelani and M. Molinas, "Optimal use of power electronic interfaces for loads in distributed systems," in *Proc. IEEE ISIE*, 2010, pp. 2449–2454.
[13] N. Jelani and M. Molinas, "Stability investigation of control system for power electronic converter acting as load interface in AC distribution systems," in *Proc. IEEE ISIE*, 2011, pp. 408–413.
[14] B. Singh, R. Saha, A. Chandra, and K. Al-Haddad, "Static synchronous compensators (STATCOM): A review," *IET Power Electron.*, vol. 2, no. 4, pp. 297–324, Jul. 2009.
[15] M. N. Slepchenkov, K. M. Smedley, and J. Wen, "Hexagram-converter-based STATCOM for voltage support in fixed-speed wind turbine generation systems," *IEEE Trans. Ind. Electron.*, vol. 58, no. 4, pp. 1120–1131, Apr. 2011.
[16] S. R. Pulikanti and V. G. Agelidis, "Hybrid flying-capacitor-based active-neutral-point-clampled five-level converter operated with SHE-PWM," *IEEE Trans. Ind. Electron.*, vol. 58, no. 10, pp. 4643–4653, Oct. 2011.
[17] M. Molinas, J. A. Suul, and T. Undeland, "Extending the life of gear box in wind generators by smoothing transient torque with STATCOM," *IEEE Trans. Ind. Electron.*, vol. 57, no. 2, pp. 476–484, Feb. 2010.
[18] P. Sharma and T. Bhatti, "Performance investigation of isolated wind-diesel hybrid power systems with WECS having PMIG," *IEEE Trans. Ind. Electron.*, vol. 60, no. 4, pp. 1630–1637, Apr. 2013.
[19] S. Anand, B. G. Fernandes, and K. Chatterjee, "DC voltage controller for asymmetric-twin-converter-topology-based high-power STATCOM," *IEEE Trans. Ind. Electron.*, vol. 60, no. 1, pp. 11–19, Jan. 2013.
[20] C.-H. Liu and Y.-Y. Hsu, "Design of a self-tuning PI controller for a STATCOM using particle swarm optimization," *IEEE Trans. Ind. Electron.*, vol. 57, no. 2, pp. 702–715, Feb. 2010.
[21] W. Song and A. Q. Huang, "Fault-tolerant design and control strategy for cascaded H-bridge multilevel converter-based STATCOM," *IEEE Trans. Ind. Electron.*, vol. 57, no. 8, pp. 2700–2708, Aug. 2010.
[22] C. A. Sepulveda, J. A. Munoz, J. R. Espinosa, M. E. Figueroa, and P. E. Melin, "All-on-chip *dq*-frame based D-STATCOM control implementa-tion in a low-cost FPGA," *IEEE Trans. Ind. Electron.*, vol. 60, no. 2, pp. 659–669, Feb. 2013.
[23] C. Han, A. Huang, M. Baran, S. Bhattacharya, W. Litzenberger, L. Anderson, A. Johnson, and A. A. Edris, "STATCOM impact study on the integration of a large wind farm into a weak loop power system," *IEEE Trans. Energy Convers.*, vol. 23, no. 1, pp. 226–233, Mar. 2008.
[24] M. Molinas, J. A. Suul, and T. Undeland, "Low voltage ride through of wind farms with cage generators: STATCOM versus SVC," *IEEE Trans. Power Electron.*, vol. 23, no. 3, pp. 1104–1117, May 2008.
[25] J. Suul, M. Molinas, and T. Undeland, "STATCOM-based indirect torque control of induction machines during voltage recovery after grid faults," *IEEE Trans. Power Electron.*, vol. 25, no. 5, pp. 1240–1250, May 2010.
[26] A. Yazdani, H. Sepahvand, M. L. Crow, and M. Ferdowsi, "Fault detection and mitigation in multilevel converter STATCOMs," *IEEE Trans. Ind. Electron.*, vol. 58, no. 4, pp. 1307–1315, Apr. 2011.
[27] K. Li, J. Liu, Z. Wang, and B. Wei, "Strategies and operating point optimization of STATCOM control for voltage unbalance mitigation in three-phase three-wire systems," *IEEE Trans. Power Del.*, vol. 22, no. 1, pp. 413–422, Jan. 2007.
[28] T. Lee, S. Hu, and Y. Chan, "D-STATCOM with positive-sequence admittance and negative-sequence conductance to mitigate voltage fluctuations in high-level penetration of distributed generation systems," *IEEE Trans. Ind. Electron.*, vol. 60, no. 4, pp. 1417–1428, Apr. 2013.
[29] M. Castilla, J. Miret, A. Camacho, J. Matas, E. Alarcón-Gallo, and L. Garcıacute;a de Vicuña, "Coordinated reactive power control for static synchronous compensators under unbalanced voltage sags," in *Proc. IEEE ISIE*, 2012, pp. 987–992.
[30] P. Rodrıacute;guez, G. Medeiros, A. Luna, M. C. Cavalcanti, and R. Teodorescu, "Safe current injection strategies for a STATCOM under asymmetrical grid faults," in *Proc. IEEE ECCE*, 2010, pp. 3929–3935.
[31] P. Rodrıacute;guez, A. Luna, R. Munoz-Aguilar, F. Corcoles, R. Teodorescu, and F. Blaabjerg, "Control of power converters in distributed generation applications under grid fault conditions," in *Proc. IEEE ECCE*, 2011, pp. 2649–2656.
[32] E. Figueres, G. Garcerá, J. Sandia, F. González-Espin, and J. Calvo, "Sensitivity study of the dynamics of three-phase photovoltaic inverters with an LCL grid filter," *IEEE Trans. Ind. Electron.*, vol. 56, no. 3, pp. 706–717, Mar. 2009.
[33] M. Liserre, R. Teodorescu, and F. Blaabjerg, "Stability of photovoltaic and wind turbine grid-connected inverters for a large set of grid impedance values," *IEEE Trans. Power Electron.*, vol. 21, no. 1, pp. 263–272, Jan. 2006.
[34] G. Shen, X. Zhu, J. Zhang, and D. Xu, "A new feedback method for PR current control of LCL-filter-based grid-connected inverter," *IEEE Trans. Ind. Electron.*, vol. 57, no. 6, pp. 2033–2041, Jun. 2010.
[35] D. N. Zmood and D. G. Holmes, "Stationary frame current regulation of PWM inverters with zero steady-state error," *IEEE Trans. Power Electron.*, vol. 18, no. 3, pp. 814–822, May 2003.
[36] A. G. Yepes, F. D. Freijedo, J. Doval-Gandoy, O. Lopez, J. Malvar, and P. Fernandez-Comesana, "Effects of discretization methods on the performance of resonant controllers," *IEEE Trans. Power Electron.*, vol. 25, no. 7, pp. 1692–1712, Jul. 2010.
[37] P. Rodriguez, A. Luna, I. Candela, R. Mujal, R. Teodorescu, and F. Blaabjerg, "Multiresonant frequency-locked loop for grid synchronization of power converters under distorted grid conditions," *IEEE Trans. Ind. Electron.*, vol. 58, no. 1, pp. 127–138, Jan. 2011.
[38] G. Yaleinkaya, M. H. J. Bollen, and P. A. Crossley, "Characterization of voltage sags in industrial distribution systems," *IEEE Trans. Ind. Appl.*, vol. 34, no. 5, pp. 682–688, Jul./Aug. 1998.
[39] M. H. J. Bollen, "Algorithms for characterizing measured three-phase unbalanced voltage dips," *IEEE Trans. Power Del.*, vol. 18, no. 3, pp. 937–944, Jul. 2003.
[40] *IEEE Standard for Interconnecting Distributed Resources with Electric Power Systems*, IEEE Std. 1547.2-2008, 2009.
[41] S. Cundeva, R. Neumann, M. Bollen, Z. Kokolanski, J. Vuletic, A. Krkoleva, S. Djokic, K. van Reusel, and K. Stockman, "Immunity against voltage dips—Main recommendations to stakeholders of the CIGRE/CIRED/UIE joint working group C4.110," *Int. J. Emerg. Sci.*, vol. 1, no. 4, pp. 555–563, Dec. 2011.

Miguel Castilla received the B.S., M.S., and Ph.D. degrees in telecommunication engineering from the Technical University of Catalonia, Barcelona, Spain, in 1988, 1995, and 1998, respectively.

Since 2002, he has been an Associate Professor with the Department of Electronic Engineering, Technical University of Catalonia, where he teaches courses on analog circuits and power electronics. His research interests include power electronics, nonlinear control, and renewable energy systems.

Jaume Miret (M'98) received the B.S. degree in telecommunications, the M.S. degree in electronics, and the Ph.D. degree in electronics from the Technical University of Catalonia, Barcelona, Spain, in 1992, 1999, and 2005, respectively.

Since 1993, he has been an Assistant Professor with the Department of Electronic Engineering, Technical University of Catalonia, where he teaches courses on digital design and circuit theory. His research interests include dc-to-ac converters, active power filters, and digital control.

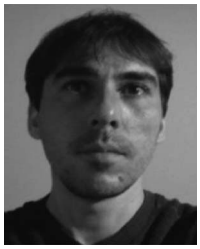

Antonio Camacho received the B.S. degree in chemical engineering and the M.S. degree in automation and industrial electronics from the Technical University of Catalonia, Barcelona, Spain, in 2000 and 2009, respectively. He is currently working toward the Ph.D. degree in electronic engineering at the Technical University of Catalonia.

His research interests include networked and embedded control systems, industrial informatics, and power electronics.

José Matas received the B.S., M.S., and Ph.D. degrees from the Technical University of Catalonia, Barcelona, Spain, in 1988, 1996, and 2003, respectively, all in telecommunications engineering.

From 1988 to 1990, he was an Engineer with a consumer electronics company. Since 1990, he has been an Associate Professor with the Department of Electronic Engineering, Technical University of Catalonia. His research interests include power-factor-correction circuits, active power filters, uninterruptible power systems, distributed power systems, and nonlinear control.

Luis García de Vicuña received the Ingeniero de Telecomunicación and Dr.Ing. degrees from the Technical University of Catalonia, Barcelona, Spain, in 1980 and 1990, respectively, and the Dr.Sci. degree from the Université Paul Sabatier, Toulouse, France, in 1992.

From 1980 to 1982, he was an Engineer with a control applications company. He is currently a Professor with the Department of Electronic Engineering, Technical University of Catalonia, where he teaches courses on power electronics. His research interests include power electronics modeling, simulation and control, active power filtering, and high-power-factor ac/dc conversion.